



Article

Path Loss Determination Using Linear and Cubic Regression Inside a Classic Tomato Greenhouse

Dora Cama-Pinto ^{1,*}, Miguel Damas ¹, Juan Antonio Holgado-Terriza ²,
Francisco Gómez-Mula ¹ and Alejandro Cama-Pinto ³

¹ Department of Computer Architecture and Technology, University of Granada, 18071 Granada, Spain; mdamas@ugr.es (M.D.); frgomez@ugr.es (F.G.-M.)

² Software Engineering Department, University of Granada, 18071 Granada, Spain; jholgado@ugr.es

³ Department of Computer Sciences and Electronic, Universidad de la Costa, Barranquilla 080002, Atlantico, Colombia; acama1@cuc.edu.co

* Correspondence: doracamapinto@correo.ugr.es; Tel.: +49-157-7643-1276

Received: 21 March 2019; Accepted: 14 May 2019; Published: 17 May 2019



Abstract: The production of tomatoes in greenhouses, in addition to its relevance in nutrition and health, is an activity of the agroindustry with high economic importance in Spain, the first exporter in Europe of this vegetable. The technological updating with precision agriculture, implemented in order to ensure adequate production, leads to a deployment planning of wireless sensors with limited coverage by the attenuation of radio waves in the presence of vegetation. The well-known propagation models FSPL (Free-Space Path Loss), two-ray, COST235, Weissberger, ITU-R (International Telecommunications Union—Radiocommunication Sector), FITU-R (Fitted ITU-R), offer values with an error percentage higher than 30% in the 2.4 GHz band in relation to those measured in field tests. As a substantial improvement, we have developed optimized propagation models, with an error estimate of less than 9% in the worst-case scenario for the later benefit of farmers, consumers and the economic chain in the production of tomatoes.

Keywords: propagation model; wireless propagation model; precision agriculture; COST235; ITU-R; FITU-R; Weissberger model

1. Introduction

The Food and Agriculture Organization of the United Nations (FAO) predicts that the world population will reach 8 billion people by 2025 and 9.6 billion by 2050 [1]. One of the most promising concepts, which is expected to contribute greatly to the necessary increase in food production in a sustainable manner, is precision agriculture (PA) [2,3]; a set of technologies used to understand changes during planting cycles. Precision agriculture arises from the need for technologies to collect information in agricultural areas about soil conditions from the environment and transmit data. It offers the means for agricultural practices to be monitored, evaluated and controlled. This information directly affects the decision-making on the activities to be carried out throughout the plantation.

The PA relies on applications of wireless sensor networks (WSN) in the function of monitoring and controlling the management of a field because it reduces the costs of monitoring and managing crop production at the plant level, instead of monitoring the entire greenhouse [4–9] or with the purpose to make environmental measurements (i.e., on water or soil) [10]. In PA, the deployment of WSN has provided greater financial returns by optimizing product quality and quantity of yield while minimizing costs [11–14]. Therefore, in this paper we focus on studying and comparing the phenomenon of propagation and attenuation of radio waves in the unlicensed band of 2425 MHz; the most commonly used in the world of precision agriculture [3] inside the tomato production greenhouse.

Background

The surface of greenhouses in the world exceeds 700,000 ha, being concentrated mainly in Asia, in the Mediterranean basin, and in central and northern Europe [15]. In this order of ideas, world exports of tomatoes exceeded 6.9 billion euros in 2013, with the EU, the main sector of world trade in fresh tomatoes, with 57.8% in 2013 (volume in kg) and 65.7% of turnover (volume in euros). Spain is the main supplier, with 23.78% and 21.7% of EU imports in tons and euros respectively. Of the 27,000 ha of greenhouses in the province of Almería, 10,232 ha are destined to fresh tomato crops, the main crop in the greenhouses of Almería with a total production of 958,462 tons, which represents 83.2% of the surface and 61% of the total production of Andalusia having the first place in the national production. Regarding exports, its main markets are in the EU, especially Germany, France, the Netherlands and the United Kingdom [16,17]. Due to this relevance, our research is focused on tomato greenhouses. Accordingly, the most widespread empirical propagation models in the presence of vegetation are those shown in Table 1. However, because they are general, the predictions that the aforementioned models show could be improved with values closer to the real ones, helping to contribute to better planning in the deployment being this the main object of our study.

According to the literature reviewed we have found similar research that studies the influence of foliage on radio path losses for WSN planning orchards [18] and a study that improves the path loss model for wireless sensor networks in mango greenhouses [19], others based on deployment of WSN over tomato greenhouses for monitoring environmental variables [20], and precision agriculture [21], but none of the reviewed literature was related to radio wave propagation models for tomato production greenhouse as in our work.

2. Materials and Methods

2.1. The Wireless Sensor Network

Wireless sensor networks (WSN) are one of the most important technologies of the 21st century [22] being an optimized form of acquisition and transmission of information [23], overcoming deployment difficulties and high installation and maintenance costs [24]. Wirelessly, a network can be quickly built automatically, using hierarchical network communication protocols and distributed algorithms. On the other hand, given that the nodes of the sensors are small in size and have a good capacity for cooperation, their deployment has a small impact on the agricultural environment. They also have other advantages, such as low energy consumption, self-organization capacity and local processing, constituting a promising platform for the implementation of monitoring systems that are increasingly used in agriculture [25–30].

The WSN in our study is based on the IEEE 802.15.4 standard, operating in the 2.4 GHz band, has lower width of the Fresnel zones compared to the 868, 915 MHz bands and with a faster transmission speed [6]. It is an important tool for environmental monitoring [31,32], and its use in rural areas and in the presence of vegetation is growing exponentially [33,34]. It establishes communication and detection infrastructures in areas where, otherwise, it would be impractical or impossible to do so [35]. However, each sensor used in the WSN has a limited scope [36]. Therefore, to efficiently plan and deploy WSNs in the presence of vegetation, it is crucial to have knowledge of the position, the level of transmission power and the propagation of the radio signal in the deployment environment [37]. The attenuation of the propagated signal increases with distance [38], and in areas of dense vegetation, such as orchards and forests, where the line of sight (LOS) between the nodes is typically non-existent, the foliage of trees may cause additional attenuation [39] by diffraction, reflection and scattering if there is no line of sight (NLOS) [40], especially due to the presence of water within the leaves and stems [41].

2.2. Received Signal Strength Indicator (RSSI)

The intensity of the received signal (RSSI—received signal strength indicator) is used to know the propagation of the radio wave [42–44]. The surrounding environment, the growth of crops and the

different antenna heights will influence the measurement of RSSI [37]. In that sense, the models used to predict the RSSI between two transceivers are called propagation models [45].

2.3. Propagation with Line of Sight

1. Loss in free space. When an electromagnetic wave (EM) propagates in free space, path loss can be calculated using the Friis equation, widely used by microwave link designers [42], which assumes the absence of obstacles in the vicinity [39,46]: $\frac{P_r}{P_t} = \left(\frac{4\pi fd}{c}\right)^2$, where P_r and P_t are the receiver and transmitter power respectively, f is the frequency of the radiation wave, c , the speed of light in the vacuum and d is the distance between the transmitter and the receiver [36,47]. The loss of the path in the free space means that the transceiver antennas, both transmitters and receivers, use communication with LOS, without obstructions or reflections of any kind. However, if the antennas are located close to the ground, the above equation is no longer valid, the reflection of the earth must be taken into account [18]. The power loss is usually expressed in terms of “path loss” (PL), defined as: $PL = 10\log_{10}(P_t/P_r)$ [48] with P_t and P_r as power transmitted and received, respectively. Therefore, PL in free space can be expressed: $PL_{\text{Free-space}}(\text{dB}) = 20\log(f) + 20\log(d) - 147.56$, the radiofrequency, f , is expressed in Hz and distance is expressed in meters [49,50].
2. Two-ray propagation model. When the RF propagates near the ground with LOS, the flat ground wave (PE) propagation model can be used to define the path loss instead of the $PL_{\text{Free-space}}$ model. This model includes the effects of the reflection of the rays of the ground and the ray LOS, which is given by the equation: $PL_{\text{PE}}(\text{dB}) = 40\log(d) - 20\log(h_T) - 20\log(h_R)$, where d is the distance between the transmitter and receiver antennas in meters, h_T and h_R are the elevations of the transceiver antennas in meters. The separation distance (d) in this model is much greater than h_T and h_R [45].

2.4. Total Loss

Signals at millimeter wave and microwave frequencies experience scattering and absorption caused by leaves and branches of vegetation randomly distributed [51]. Therefore, the total path losses are formulated by combining the losses of the $PL_{\text{Free-space}}$ model with the PL_{veg} vegetation losses that are predicted by the different vegetation models: $PL_{\text{tot}} = PL_{\text{Free-space}} + PE_{\text{veg}}$, where PL_{tot} is the total path loss [4].

2.5. Link Budget

The link budget is used to obtain the signal strength in the receiver, considering all the losses in the path between the transmitter and the receiver. The received power, which represents all the gains and losses is defined by the equation: $P_r(\text{dBm}) = P_t + G_t + G_r - L_{\text{path}}$, where P_r and P_t are the power received and transmitted. G_t and G_r are the gains of the transmitter and receiver; L_{path} is the total path loss [5].

2.6. Propagation with Non Line of Sight (NLOS)

It is important to study the effects of vegetation on a signal because many applications require the use of the microwave frequency band (0.3–300 GHz). In addition, depending on the thickness of the vegetation and the frequency of operation, a signal could travel along diffracted trails reducing the range of radio equipment communications. Quantitative knowledge of the excess of propagation loss suffered by radio waves due to the presence of vegetation is essential to plan a communication link in any wooded land [52–55]. Inside a greenhouse, in addition to attenuation in free space, electromagnetic waves are vanished by mechanisms that include diffraction, reflection, and dispersion produced by the leaves, branches, and stems of crops, distributed at random, between the transmitter and receiver, having an unknown effect on the exact propagation of radio waves (see Figure 1) [56]. To determine

these changes, propagation models are used that estimate the radio coverage area of a transmitter and show the strength of the signal between the transmitter and receiver [11,12,36,57].

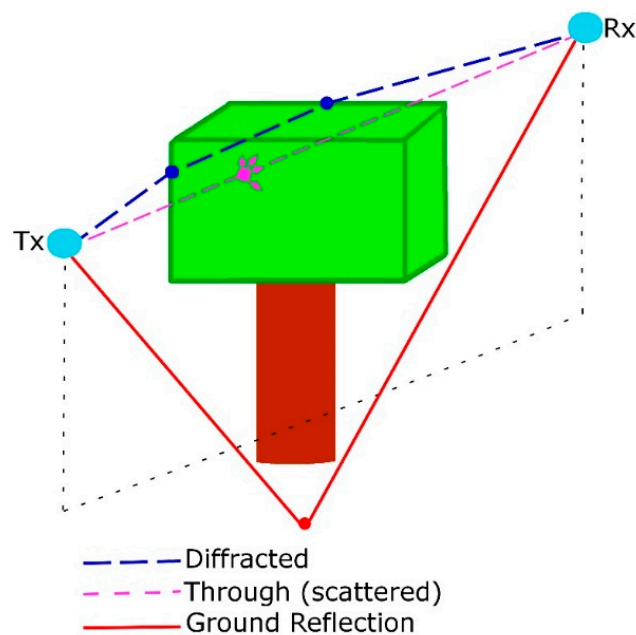


Figure 1. Possible mechanisms of propagation in the presence of vegetation.

2.7. Propagation Model

Propagation models to predict the excess attenuation produced by vegetation were developed to model the excess attenuation found in a forest beyond what is predicted by free space or two-ray propagation [58]. These models can be theoretical and empirical. Theorists or analysts require a large database of environmental characteristics, requiring knowledge of parameters such as electromagnetic, soil moisture and leaves, geometrical characteristics, etc., which may be impractical and therefore we do not use it in our investigation. On the other hand, the empirical path loss models are based on actual radio frequency (RF) measurements of wireless channels [19]. Their main advantages over theoretical path loss models is the simplicity of the mathematical expressions applied that facilitate their direct application, their ease of implementation and their ability to include a greater environment-related factors that affect the propagation of radio waves. However, they do not take into account the geometry of the site [25,45,58–60]. Within the models of empirical propagation, there is the model of exponential decay proposed by Weissberger (1982), the model COST235 (1996) that considered the situation of trees with leaves and without it. Additionally to Recommendation ITU-R (CCIR 1986), Al-Nuaimi and Stephens (1998) proposed the FITU-R model. Each of the models used in the development of the research is summarized in Table 1 [61–72].

The Weissberger model expresses the excess attenuation (dB) of an obstacle in the propagation path. It is applicable in situations in which propagation is likely to occur through a grove and not by diffraction on the tree crown [37,66,72]. The basic model MED (Modified Exponential Decay) is described as $Att_{MED} = Xf^Y d^Z$, where f is the frequency in megahertz (MHz), d is the depth of the vegetation in meters and X , Y and Z are parameters adjusted by techniques of regression [59]. In that sense, the intensity of the received signal (RSSI) for wireless systems in vegetation media is largely based on empirical models that are relatively easy to use [73].

Table 1. Empirical propagation models.

| Model | Equation |
|---|---|
| The modified exponential decay model of Weissberger | $L_{\text{Weiss}} = 0.45f^{0.284}d, 0 \text{ m} < d < 14 \text{ m}$ $L_{\text{Weiss}} = 1.33f^{0.284}d^{0.558}, 14 \text{ m} < d < 400 \text{ m}$ The frequency f in GHz and the depth of the trees, d , in meters. Applicable at frequencies of 0.23–95 GHz. |
| Loss factor of the ITU-R model | $L_{\text{ITU-R}} = 0.2f^{0.3}d^{0.6}, d < 400 \text{ m.}$ The frequency f in MHz and the depth of the trees, d , in meters. Applicable to the frequency of 0.2–95 GHz. |
| Loss factor of the COST235 model | $L_{\text{COST235}} = 26.6f^{-0.2}d^{0.5} \text{ out-of-leaf}$ $L_{\text{COST235}} = 15.6f^{-0.009}d^{0.26} \text{ in-leaf}$ f is the transmission frequency (MHz), d is the depth of the trees in meters. Applicable to the frequency of 0.2–95 GHz |
| FITU-R | $L_{\text{FITU-R}} = 0.37f^{-0.18}d^{0.59} \text{ out-of-leaf}$ $L_{\text{FITU-R}} = 0.39f^{-0.39}d^{0.25} \text{ in-leaf}$ f is the frequency in MHz and d is the tree depth in meter, based on millimeter VHF wave measurement data on a short foliage depth (maximum of 400 m) |

2.8. Hardware

1. Raspberry Pi. The Raspberry Pi 3 computer receives data from the sensor node through the sink node connected to its USB port. The electric energy, available inside the greenhouse, fed the Raspberry Pi uninterruptedly during the testing stage.
2. Sensor and sink nodes. We used the Re-Mote nodes [74] that operate with the 2.4 GHz band (CC2538 System-on-Chip) for both the sensor node and the sink. The sink node is powered by the power provided by the USB cable connected to the Raspberry Pi computer (See Figure 2A), while the sensor node has a rechargeable Lithium-ion battery of 3.7 V and 6600 mAh (See Figure 2B).

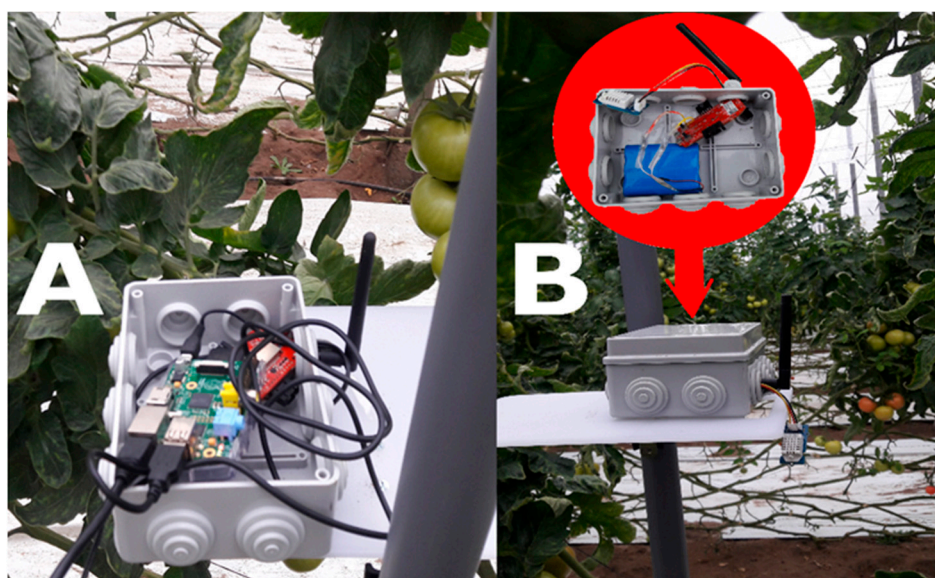


Figure 2. Wireless sensor networks (WSN) nodes. (A) Sink node connected to the Raspberry Pi. (B) Sensor node powered by an external lithium battery.

2.9. Software

The Contiki operating system has been used in the wireless nodes. The applications were written in programming language C so that the sensor node sends information to the sink node, and it receives it and forwards it to the embedded computer (Raspberry Pi). The sensor node is programmed

to save energy consumption so that its radio module at 2.4 GHz is not active all the time, giving greater durability to the lithium-ion battery while the sink node is constantly fed from the computer. The Raspberry Pi works with the Raspbian operating system, and through a script written in Python, it collects the information from the sink node in its USB port and then stores it in CSV format in its μ SD memory.

2.10. Test Environment

The tests were carried out in February 2018 inside four Tinkwino tomato greenhouse, each one an area of 10,000 m² whose production is marketed in the European market. It is located in the Cañada de San Urbano, province of Almería, autonomous community of Andalusia in Spain. The distribution of the plantation is the classic one for a greenhouse of tomato, with corridors of 1.2 m (Figure 3B), 50 cm of distance between plants (Figure 3C), separation between paired lines and ends of the foliagees 60 and 100 cm respectively (Figure 3D), and with a length of the main hall being 100 m (Figure 3E).

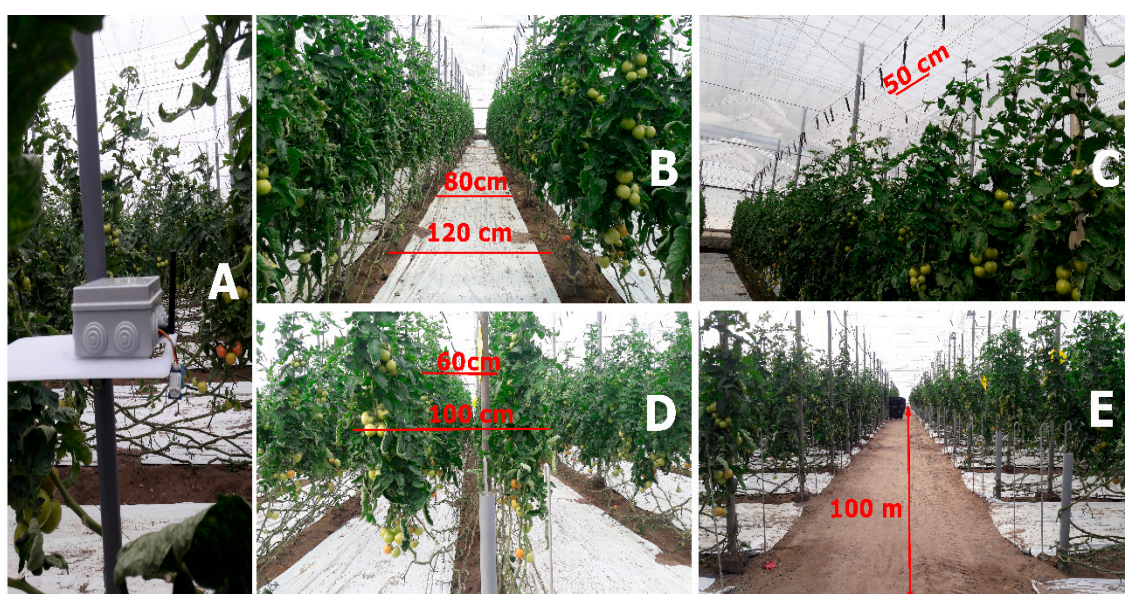


Figure 3. Internal view of the tomato greenhouse in Almería. (A) Sensor node, (B) aisle dimensions, (C) distance between floors, (D) separation of paired lines, (E) main hallway measurement.

2.11. Field Tests

The WSN network was deployed in the greenhouse following the distribution of Figure 4A,B. The mast that supports each node has a base of 17 kg to give stability and avoid possible rocking. The sink node (red color) and sensor (light blue) were initially in positions A1 and B1 respectively at the same height. The data sink with RSSI information in dBm were sent every 10 s for 10 min, arrived at the sink node. After completing the RSSI data collection, these were moved 2 m to the right (A2, A3, A4 and B2, B3, B4), and the average in the four positions was recorded. This process was repeated again at a different height. Later the sensor node moved from position Bx to Cx and so on as long as there was connectivity with the sink Ax located at the end of the greenhouse lacking line of sight. Finally, we elaborated the measurement curve and contrasted it with the propagation models of radio waves in the presence of vegetation.

In the literature reviewed, transceiver transmission power and antenna gains were assumed to be those in the technical sheets, and these data were used to calculate the propagation loss later. However, these were far from real and altered the accuracy of subsequent estimates. For this reason, through field tests, the real value of the transmit power was measured so that the results were reliable.

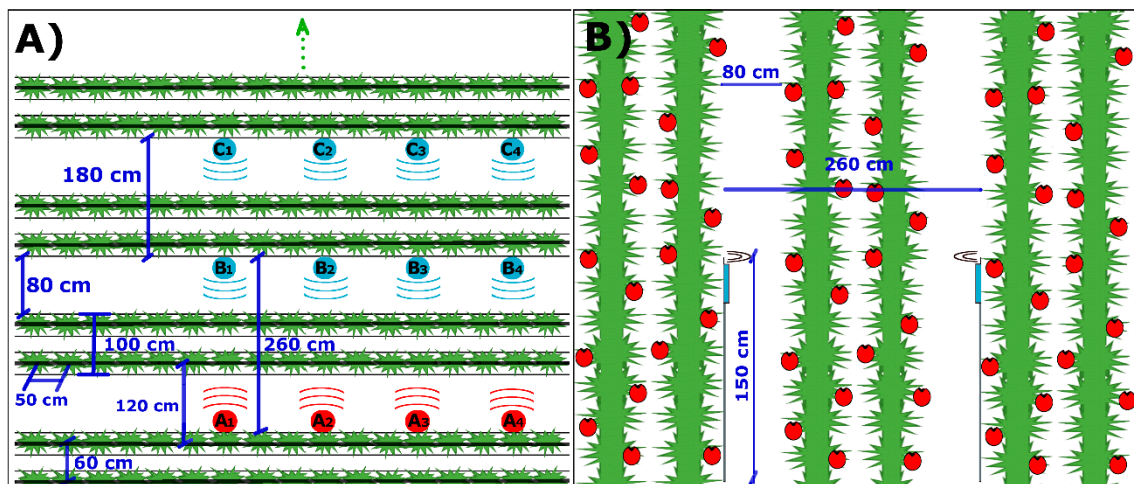


Figure 4. Tomato greenhouse diagram and WSN deployment layout in the tests. (A) View from above, (B) transverse view.

3. Results and Discussions

During the field-tests, omnidirectional antennas were used in each node because they were traditionally used on agricultural deployments for WSN devices for the purpose of cover links P2MP (point-to-multipoint communication) and MP2MP (multi-point to multi-point) in a real solution. The height of the transmitter and receiver omnidirectional antennas during the tests carried out inside the greenhouse were 30 cm, 50 cm, 70 cm, 90 cm, 100 cm, 150 cm, and 200 cm from the ground. Based on the power levels recorded at the receiving node, the largest and smallest measured ranges were when the antenna height of the transmitting node (Tx) and receiver (Rx) were both 0.5 m and 1.5 m respectively using the 2.4 GHz band (Figure 5).

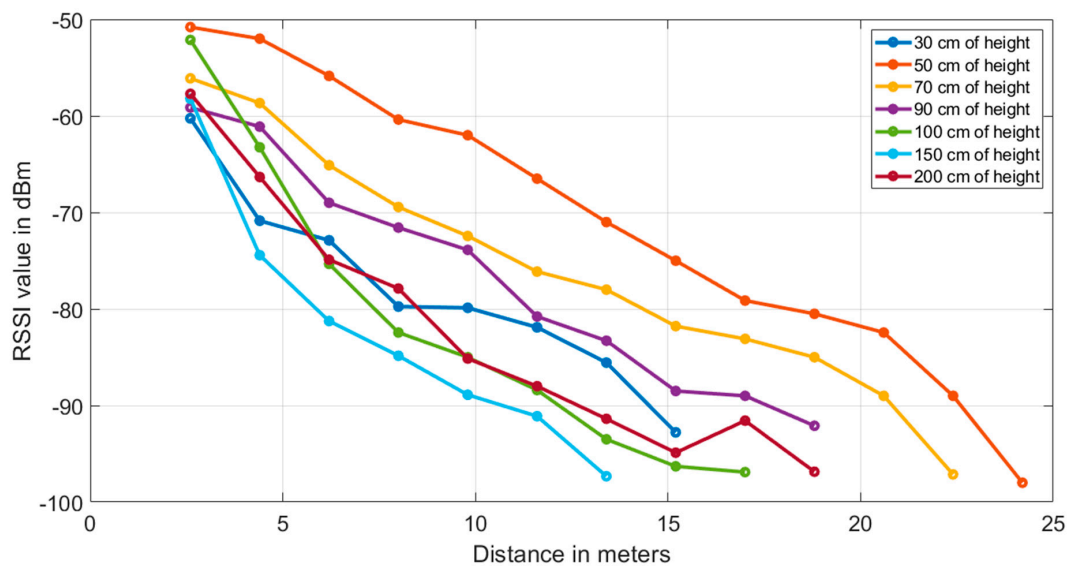


Figure 5. Signal level in dBm and maximum coverage between the transmitting node (Tx) and receiver (Rx) node at different heights with respect to the ground (30 cm, 50 cm, 70 cm, 90 cm, 100 cm, 150 cm, and 200 cm).

Table 2 compares the attenuation values in the greenhouse (empirical PL) with respect to the separation distance of the nodes Tx and Rx measured in meters, when they were located 0.5 m and 1.5 m above the ground. The separations between the nodes were initially 2.6 m and then increased steadily by 1.8 m due to the plantation frame that has the scheme of Figure 4. The variations of the values in the attenuations were due to the conformation in the structure of the vegetation different heights. On average, in our case study, the highest density in vegetation consisting of stems, leaves and fruits was at a height of 1.5 m.

Table 2. Total attenuation of the propagation of the radio wave in the presence of vegetation with nodes at 0.5 m and 1.5 m from the ground.

| Model | Distance (m) | | | | | | | | | | | | |
|----------------------------|--------------|-------|-------|-------|-------|-------|-------|------|-------|------|-------|------|------|
| | 2.6 | 4.4 | 6.2 | 8 | 9.8 | 11.6 | 13.4 | 15.2 | 17.0 | 18.8 | 20.6 | 22.4 | 24.2 |
| Empirical PL (dB) at 0.5 m | 26.8 | 28 | 31.86 | 36.38 | 38 | 42.5 | 47 | 51 | 55.13 | 56.5 | 58.44 | 65 | 74 |
| Empirical PL (dB) at 1.5 m | 34.22 | 50.43 | 57.25 | 60.85 | 64.89 | 70.11 | 73.33 | - | - | - | - | - | - |

With the Tx and Rx nodes at 0.5 m from the ground, the results obtained in the field tests were compared with the models with LOS (Line of Sight), the FSPL (Free-Space Path Loss) and two-ray with the graphs of curves shown in Figure 6A. In addition, the COST235, FITU-R, ITU-R, and Weissberger models were added to the losses of the unobstructed path corresponding to the corridors and spaces between floors with the FSPL and two-ray models in 6B and 6C respectively. From all these graphs it was concluded that the closest models were two-ray and Weissberger, adding the attenuation of two-ray. Analogously it is the analysis in Figure 7A–C working with the nodes Tx and Rx at 1.5 m above the ground.

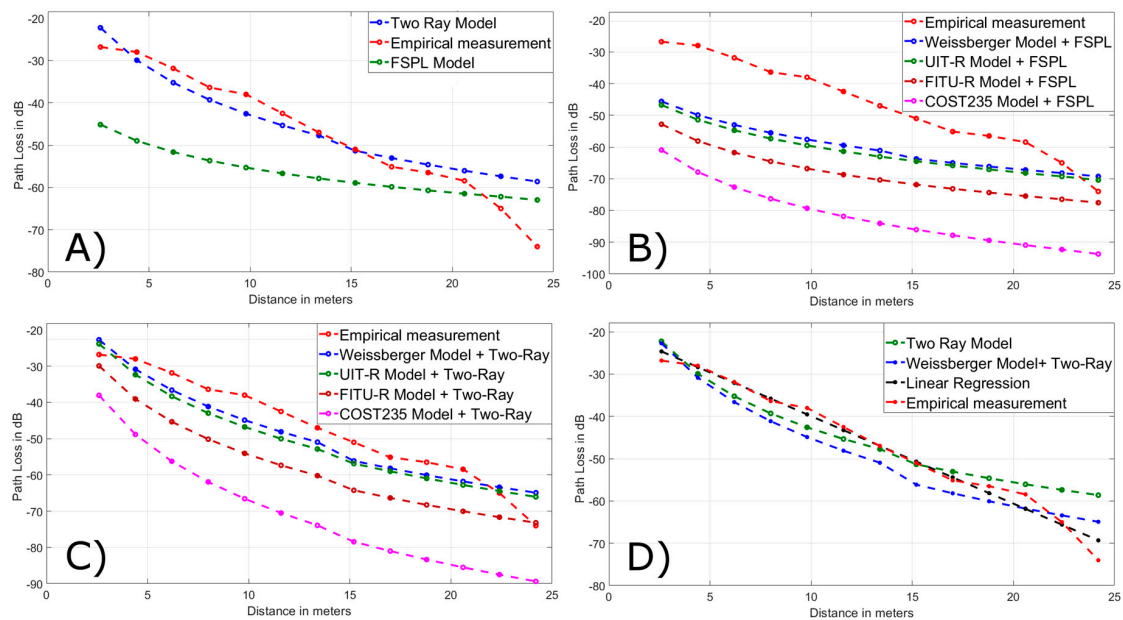


Figure 6. Field measurement at 0.5 m of soil vs. (A) models with line of sight (LOS), (B) empirical models + FSPL, (C) empirical models + two-ray, (D) optimized model (linear regression) and the others closest in values.

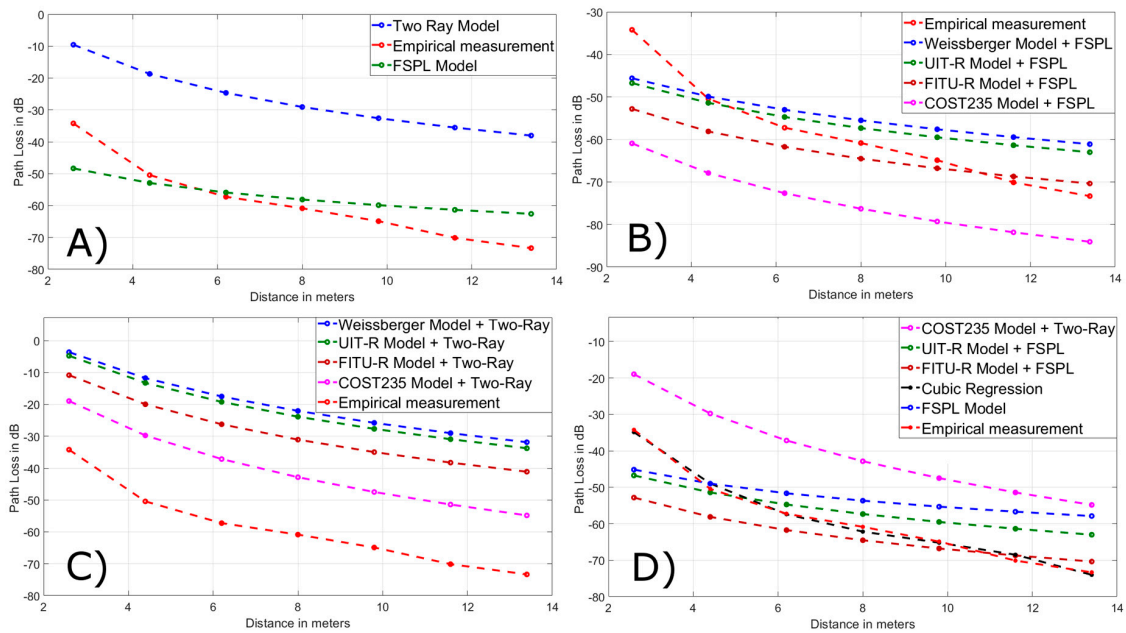


Figure 7. Field measurement at 1.5 m of soil vs. (A) models with LOS (B), empirical models + FSPL (C), empirical models + two-ray, (D) optimized model (cubic regression) and the others closest in values.

New Optimized Model with Verification of Values

The Matlab program (R2018a) has been used to develop our optimized model through linear regression when the nodes were at 0.5 m from the ground. The mathematical equation used was: $y = -2.0685d - 19.252$ (where d is the distance between the nodes T_x and R_x). If the nodes T_x and R_x are placed at a 1.5m distance from the ground, the mathematical equation of the optimized model was obtained by cubic regression using the same software is this time: $y = -0.056156d^3 + 1.6125d^2 - 17.006d - 0.56299$. The Figures 6D and 7D show the best precision of our models with respect to the others. The other models with the closest approximation of values were two-ray and Weissberger a 0.5 m and COST235, UIT-R, FITU-R, FSPL for 1.5 m. Likewise, the percentage of error (% error) was found with the following formula: $Abs\{[1 - (X_{i\text{ empirical}}/X_{i\text{ model}})] \times 100\%$, where X_i is the measured value ($X_{i\text{ empirical}}$) or predicted ($X_{i\text{ model}}$) in a specific distance. In our models, they were less than 9%, better than the other models, and are corroborated in Figure 8, with the variability of each proposed model in relation to empirical measurement values. The Tables 3 and 4 in the shaded records validate the optimization of the equations.

Regardless of the brand or model of the sensor node, with the developed models it is possible to plan the maximum distance that two nodes can be separated knowing the reception sensitivity and the EIRP (effective isotropic radiated power) and from there if you want to expand the coverage you could do it with a multi-hop topology. For example, the signal sent from the transmitter node was attenuated through the vegetation, and was detected in the receiver with a strength of -87 dBm, being the link margin of 10 dB because the receiver sensitivity of the node was -97 dBm in our case [-87 dBm $- (-97$ dBm) = 10 dB]. There is acceptable link stability from a link margin equal to or greater than 10 dB, according [75–79]. With these described features, it is possible to link two nodes at a maximum distance of 20.6 and 13.6 m if they are at a height of 0.5 or 1.5 m, respectively. In this same example, maintaining the positions of the transmitter and receiver with other features of nodes (different brand and model), if the receiver detects -70 dBm, and the receiver sensitivity of the new node was -90 dBm, then, likewise, the distance between the two nodes could be increased until a link margin of 10 dB. Therefore, the contribution of our model is useful for the prediction of the distance between two nodes and the planning of nodes deployment.

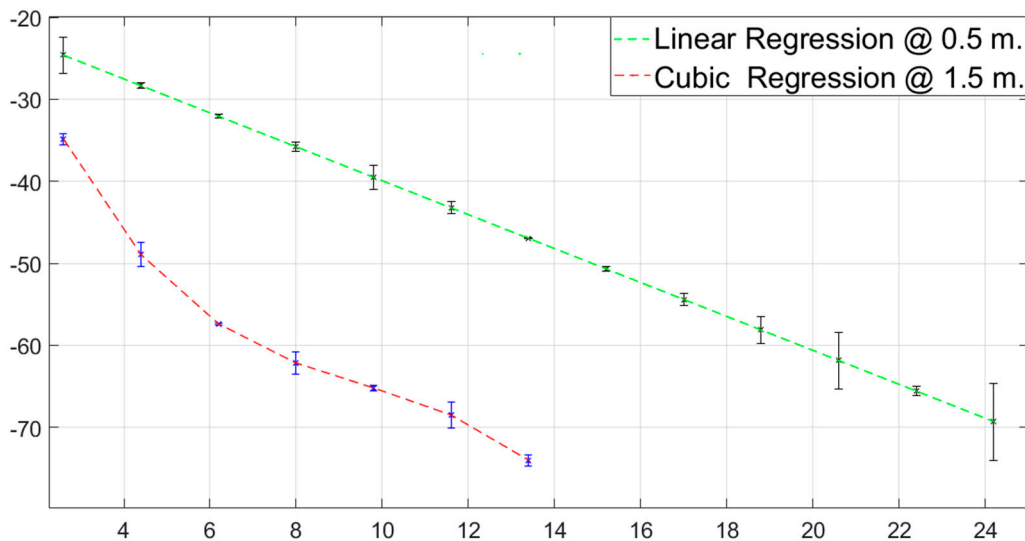


Figure 8. Linear and cubic regression for measurement at 0.5 m and 1.5 m respectively along with its deviation.

Table 3. Percentage of error in the 2.4 GHz band with propagation models in the presence of vegetation when the Tx and Rx nodes were 0.5 m above the ground.

| % Error | Distance (m) | | | | | | | | | | | | |
|-----------------------|--------------|-------|-------|-------|-------|-------|-------|-------|------|------|------|-------|-------|
| | 2.6 | 4.4 | 6.2 | 8 | 9.8 | 11.6 | 13.4 | 15.2 | 17.0 | 18.8 | 20.6 | 22.4 | 24.2 |
| FSPL | 40.64 | 42.84 | 38.30 | 32.21 | 31.30 | 25.04 | 18.81 | 13.46 | 7.92 | 6.94 | 4.95 | 4.52 | 17.52 |
| Two-Ray | 20.44 | 6.44 | 9.57 | 7.41 | 10.75 | 6.27 | 1.52 | 0.65 | 3.91 | 3.44 | 4.25 | 13.27 | 26.25 |
| Weissberger + Two Ray | 17.99 | 9.24 | 12.99 | 11.56 | 15.34 | 11.66 | 7.76 | 9.15 | 5.25 | 5.93 | 5.43 | 2.51 | 13.99 |
| Linear Regression | 8.81 | 1.25 | 0.68 | 1.62 | 3.85 | 1.73 | 0.06 | 0.61 | 1.31 | 2.82 | 5.53 | 0.89 | 6.77 |

Table 4. Percentage of error in the 2.4 GHz band with propagation models in the presence of vegetation when the Tx and Rx nodes were 1.5 m above the ground.

| % Error | Distance (m) | | | | | | |
|------------------|--------------|--------|--------|--------|-------|-------|-------|
| | 2.6 | 4.4 | 6.2 | 8 | 9.8 | 11.6 | 13.4 |
| FSPL | 29.22 | 4.69 | 2.43 | 4.72 | 8.39 | 14.31 | 17.17 |
| Two-Ray | 258.13 | 169.76 | 132.23 | 109.25 | 99.02 | 97.30 | 92.77 |
| COST235 + 2-Ray | 80.52 | 69.52 | 54.08 | 42.02 | 36.65 | 36.36 | 33.75 |
| UIT-R + FSPL | 26.79 | 1.9 | 4.62 | 6.13 | 9.05 | 14.24 | 16.37 |
| FITU-R + FSPL | 35.22 | 13.22 | 7.28 | 5.69 | 2.85 | 2.04 | 4.20 |
| Cubic Regression | 1.85 | 3.01 | 0.26 | 2.11 | 0.49 | 2.34 | 0.93 |

4. Conclusions

In the present work, a complete study of the propagation models for tomatoes greenhouses was carried out. The characteristics of tomato plantation caused an attenuation due to vegetation, and to the height, so by means of this study it has been possible to see if the theoretical propagation models adjust well to the conditions that exist in the plantations of tomatoes. With the novel mathematical models of propagation of radio waves developed, a better estimation of its attenuation can be obtained for this specific environment. In this way, the results of this study allow planning the deployment of WSN in terms of maximum distances between nodes and consequently in the number of nodes that would be used.

It is recommended to place the omnidirectional antenna at a height to half a meter above ground level because greater coverage between two nodes in the deployment can be reached. By optimizing the number of nodes required to monitoring and/or automatizing the greenhouse crop, we could reduce the cost of investment, redistributing the economic savings to reinvest it on their crops. With this height, the classical models diverge up to an error percentage of 42.84%, with the Weissberger and two-rays models being the closest empirical measurement after our proposed model.

The lowest coverage was obtained at 1.5 m, and the models that most closely approximate the empirical values were those of ITU-R, ITU-R, and FSPL that can diverge on average up to an error rate of 30%. The two models that we have developed have percentages of error lower than 9% when the nodes are at a height of less than one and a half meters, and less than 3% with a half meter of separation with the ground.

Our models are replicable and help more accurately to plan, predict coverage, and optimize the number of nodes in a network of wireless sensors operating in the 2.4 GHz band in a tomato greenhouse. Future work could examine how to generalize the model to other types of greenhouse crops. However, new tests should be carried out for other crops and different greenhouse conditions, for example, with different types of planting frames.

Author Contributions: D.C.-P.: Conceptualization, formal analysis, investigation, software, writing the original draft. M.D., J.A.H.-T. and F.G.-M.: Investigation, conceptualization, formal analysis, supervision and review & editing the manuscript. A.C.-P.: Investigation, resources, and review & editing the manuscript.

Funding: This research received fund by the Ibero-American Postgraduate University Association (AUIP).

Conflicts of Interest: The authors declare no conflicts of interest.

References

1. Razafimandimby, C.; Loscrí, V.; Vegni, A.M.; Neri, A. Efficient Bayesian communication approach for smart agriculture applications. In Proceedings of the 2017 IEEE Vehicular Technology Conference, Toronto, ON, Canada, 24–27 September 2017; pp. 1–5. [[CrossRef](#)]
2. Caicedo-Ortiz, J.G.; De-la-Hoz-Franco, E.; Morales Ortega, R.; Piñeres-Espitia, G.; Combata-Niño, H.; Estévez, F.; Cama-Pinto, A. Monitoring system for agronomic variables based in WSN technology on cassava crops. *Comput. Electron. Agric.* **2018**, *145*, 275–281. [[CrossRef](#)]
3. Tzounis, A.; Katsoulas, N.; Bartzanas, T.; Kittas, C. Internet of Things in agriculture, recent advances and future challenges. *Biosyst. Eng.* **2017**, *164*, 31–48. [[CrossRef](#)]
4. Sabri, N.; Mohammed, S.S.; Fouad, S.; Syed, A.A.; Al-Dhief, F.T.; Raheemah, A. Investigation of Empirical Wave Propagation Models in Precision Agriculture. *MATEC Web Conf.* **2018**, *150*, 06020. [[CrossRef](#)]
5. Correia, F.P.; De Alencar, M.S.; Lopes, W.T.A.; De Assis, M.S.; Leal, B.G. Propagation analysis for wireless sensor networks applied to viticulture. *Int. J. Antennas Propag.* **2017**, *2017*, 7903839. [[CrossRef](#)]
6. Yoshimura, R.; Hara, M.; Nishimura, T.; Yamada, C.; Shimasaki, H.; Kado, Y.; Ichida, M. Effect of vegetation on radio wave propagation in 920-MHz and 2.4-GHz bands. In Proceedings of the Asia-Pacific Microwave Conference (APMC), New Delhi, India, 5–9 December 2016. [[CrossRef](#)]
7. Correia, F.P.; Alencar, M.S.; Carvalho, F.B.S.; Lopes, W.T.A.; Leal, B.G. Propagation analysis in precision agriculture environment using XBee devices. In Proceedings of the SBMO/IEEE MTT-S International Microwave and Optoelectronics Conference, Rio de Janeiro, Brazil, 4–7 August 2013. [[CrossRef](#)]
8. Li, J.; Shen, C. Energy conservative Wireless Sensor Networks for black pepper monitoring in tropical area. In Proceedings of the IEEE Global High Tech Congress on Electronics (GHTCE), Shenzhen, China, 17–19 November 2013; pp. 159–164. [[CrossRef](#)]
9. Montoya, F.G.; Gomez, J.; Manzano-Agugliaro, F.; Cama, A.; García-Cruz, A.; De La Cruz, J.L. 6LoWSof: A software suite for the design of outdoor environmental measurements. *J. Food Agric. Environ.* **2013**, *11*, 2584–2586.
10. Holvoet, K.; Sampers, I.; Seynaeve, M.; Jacxsens, L.; Uyttendaele, M. Agricultural and management practices and bacterial contamination in greenhouse versus open field lettuce production. *Int. J. Environ. Res. Public Health* **2015**, *12*, 32–63. [[CrossRef](#)] [[PubMed](#)]
11. Sabri, N.; Aljunid, S.A.; Salim, M.S.; Kamaruddin, R.; Ahmad, R.B.; Malek, M.F. Path loss analysis of WSN wave propagation in vegetation. *J. Phys. Conf. Ser.* **2013**, *423*, 012063. [[CrossRef](#)]
12. Paul, B.S.; Rimer, S. A foliage scatter model to determine topology of wireless sensor network. In Proceedings of the International Conference on Radar, Communication and Computing (ICRCC), Tiruvannamalai, India, 21–22 December 2012; pp. 324–328. [[CrossRef](#)]

13. Liu, H.; Meng, Z.; Wang, M. A wireless sensor network for cropland environmental monitoring. In Proceedings of the International Conference on Networks Security, Wireless Communications and Trusted Computing (NSWCTC), Wuhan, China, 25–26 April 2009; Volume 1, pp. 65–68. [[CrossRef](#)]
14. Piñeres-Espitia, G.; Cama-Pinto, A.; De La Rosa Morrón, D.; Estevez, F.; Cama-Pinto, D. Design of a low cost weather station for detecting environmental changes. *Espacios* **2017**, *38*, 13.
15. Sánchez, J.A.; Reca, J.; Martínez, J. Water productivity in a mediterranean semi-arid greenhouse district. *Water Resour. Manag.* **2015**, *29*, 5395–5411. [[CrossRef](#)]
16. De Pablo-Valenciano, J.; Giacinti-Battistuzzi, M.A.; Tassile, V.; García-Azcárate, T. Changes in the business model for Spanish fresh tomato trade. *Span. J. Agric. Res.* **2017**, *15*, e0101. [[CrossRef](#)]
17. Marín, P.; Valera, D.L.; Molina-Aiz, F.D.; López, A.; Belmonte, L.J.; Moreno, M.A. Influence of different heating systems on the development, production and quality of a tomato crop. *ITEA Inf. Tec. Econ. Agrar.* **2016**, *112*, 375–391. [[CrossRef](#)]
18. Vougioukas, S.; Anastassiu, H.T.; Regen, C.; Zude, M. Influence of foliage on radio path losses (PLs) for Wireless Sensor Network (WSN) planning in orchards. *Biosyst. Eng.* **2013**, *114*, 454–465. [[CrossRef](#)]
19. Raheemah, A.; Sabri, N.; Salim, M.S.; Ehsan, P.; Ahmad, R.B. New empirical path loss model for wireless sensor networks in mango greenhouses. *Comput. Electron. Agric.* **2016**, *127*, 553–560. [[CrossRef](#)]
20. Mancuso, M.; Bustaffa, F. A Wireless Sensors Network for monitoring environmental variables in a tomato greenhouse. In Proceedings of the IEEE International Workshop on Factory Communication Systems (WFCS), Torino, Italy, 28–30 June 2006; pp. 107–110.
21. Erazo-Rodas, M.; Sandoval-Moreno, M.; Muñoz-Romero, S.; Huerta, M.; Rivas-Lalaleo, D.; Naranjo, C.; Rojo-álvarez, J.L. Multiparametric monitoring in equatorial tomato greenhouses (I): Wireless sensor network benchmarking. *Sensors* **2018**, *18*, 2555. [[CrossRef](#)] [[PubMed](#)]
22. Zhou, H.; Qi, H.; Banhazi, T.M.; Low, T. An integrated WSN and mobile robot system for agriculture and environment applications. In *Lecture Notes of the Institute for Computer Sciences, Social-Informatics and Telecommunications Engineering, LNICST*; Springer: Cham, Switzerland, 2014; Volume 131, pp. 30–36. [[CrossRef](#)]
23. Foerster, A.; Udugama, A.; Görg, C.; Kuladinithi, K.; Timm-Giel, A.; Cama-Pinto, A. A novel data dissemination model for organic data flows. In *Lecture Notes of the Institute for Computer Sciences, Social-Informatics and Telecommunications Engineering, LNICST*; Springer: Cham, Switzerland, 2015; Volume 158, pp. 239–252. [[CrossRef](#)]
24. Chaiwatpongsakorn, C.; Lu, M.; Keener, T.C.; Khang, S.-J. The deployment of carbon monoxide wireless sensor network (CO-WSN) for ambient air monitoring. *Int. J. Environ. Res. Public Health* **2014**, *11*, 6246–6264. [[CrossRef](#)]
25. Queiroz, D.V.; Alencar, M.S.; Gomes, R.D.; Fonseca, I.E.; Benavente-Peces, C. Survey and systematic mapping of industrial Wireless Sensor Networks. *J. Netw. Comput. Appl.* **2017**, *97*, 96–125. [[CrossRef](#)]
26. Stewart, J.; Stewart, R.; Kennedy, S. Internet of Things—Propagation modelling for precision agriculture applications. In Proceedings of the Wireless Telecommunications Symposium, Chicago, IL, USA, 26–28 April 2017. [[CrossRef](#)]
27. Zhang, H.; Li, H. Node localization technology of wireless sensor network based on RSSI algorithm. *Int. J. Online Eng.* **2016**, *12*, 51–57. [[CrossRef](#)]
28. Guo, X.-M.; Yang, X.-T.; Chen, M.-X.; Li, M.; Wang, Y.-A. A model with leaf area index and apple size parameters for 2.4 GHz radio propagation in apple orchards. *Precis. Agric.* **2015**, *16*, 180–200. [[CrossRef](#)]
29. Galvan-Tejada, G.M.; Duarte-Reynoso, E.Q.; Flores-Leal, R. Standard conditions of propagation for wireless sensor networks in an inhomogeneous vegetation environment. In Proceedings of the IEEE Antennas and Propagation Society, AP-S International Symposium (Digest), Orlando, FL, USA, 7–13 July 2013; pp. 2014–2015. [[CrossRef](#)]
30. Galvan-Tejada, G.M.; Duarte-Reynoso, E.Q. A study based on the Lee propagation model for a wireless sensor network on a non-uniform vegetation environment. In Proceedings of the IEEE Latin-America Conference on Communications (LATINCOM), Cuenca, Ecuador, 7–9 November 2012. [[CrossRef](#)]
31. Li, T.; Zhang, M.; Ji, Y.H.; Sha, S.; Jiang, Y.Q.; Li, M.Z. Management of CO₂ in a tomato greenhouse using WSN and BPNN techniques. *Int. J. Agric. Boil. Eng.* **2015**, *8*, 43–51. [[CrossRef](#)]

32. Liu, H.; Meng, Z.; Shang, Y. Sensor nodes placement for farmland environmental monitoring applications. In Proceedings of the 5th International Conference on Wireless Communications, Networking and Mobile Computing WiCOM, Beijing, China, 24–26 September 2009. [[CrossRef](#)]
33. Gay-Fernandez, J.A.; Cuinas, I. Short-term modeling in vegetation media at wireless network frequency bands. *IEEE Trans. Antennas Propag.* **2014**, *62*, 3330–3337. [[CrossRef](#)]
34. Li, Z.; Wang, N.; Hong, T. RF propagation patterns at 915 MHz and 2.4 GHz bands for in-field wireless sensor networks. *Trans. ASABE* **2013**, *56*, 787–796.
35. Haber, R.; Peter, A.; Otero, C.E.; Kostanic, I.; Ejnoui, A. A support vector machine for terrain classification in on-demand deployments of wireless sensor networks. In Proceedings of the 7th Annual IEEE International Systems Conference (SysCon), Orlando, FL, USA, 15–18 April 2013; pp. 841–846. [[CrossRef](#)]
36. De Sales Bezerra, T.; De Sousa, J.A.R.; Da Silva Eleuterio, S.A.; Rocha, J.S. Accuracy of propagation models to power prediction in WSN ZigBee applied in outdoor environment. In Proceedings of the 6th Argentine Conference on Embedded Systems (CASE), Buenos Aires, Argentina, 12–14 August 2015; pp. 19–24. [[CrossRef](#)]
37. Rao, Y.; Jiang, Z.-H.; Lazarovitch, N. Investigating signal propagation and strength distribution characteristics of wireless sensor networks in date palm orchards. *Comput. Electron. Agric.* **2016**, *124*, 107–120. [[CrossRef](#)]
38. Zhang, X.; Wu, Y.; Wei, X. Localization algorithms in wireless sensor networks using nonmetric multidimensional scaling with RSSI for precision agriculture. In Proceedings of the 2nd International Conference on Computer and Automation Engineering (ICCAE), Singapore, 26–28 February 2010; Volume 5, pp. 556–559. [[CrossRef](#)]
39. Anastassiou, H.T.; Vougioukas, S.; Fronimos, T.; Regen, C.; Petrou, L.; Zude, M.; Käthner, J. A computational model for path loss in wireless sensor networks in orchard environments. *Sensors* **2014**, *14*, 5118–5135. [[CrossRef](#)]
40. Zuniga, M.; Krishnamachari, B. Analyzing the transitional region in low power wireless links. In Proceedings of the First Annual IEEE Communications Society Conference on Sensor and Ad Hoc Communications and Networks, IEEE SECON, Santa Clara, CA, USA, 4–7 October 2004; pp. 517–526.
41. Ngandu, G.; Nomatungulula, C.; Rimer, S.; Paul, B.S.; Ouahada, K.; Twala, B. Evaluating effect of foliage on link reliability of wireless signal. In Proceedings of the IEEE International Conference on Industrial Technology, Cape Town, South Africa, 25–28 February 2013; pp. 1528–1533. [[CrossRef](#)]
42. Cama-Pinto, A.; Piñeres-Espitia, G.; Caicedo-Ortiz, J.; Ramírez-Cerpa, E.; Betancur-Agudelo, L.; Gómez-Mula, F. Received strength signal intensity performance analysis in wireless sensor network using Arduino platform and XBee wireless modules. *Int. J. Distrib. Sens. Netw.* **2017**, *13*. [[CrossRef](#)]
43. Wang, J.; Peng, Y.; Li, P. Propagation characteristics of radio wave in plastic greenhouse. In *IFIP Advances in Information and Communication Technology*; Springer: Cham, Switzerland, 2016; Volume 478, pp. 208–215. [[CrossRef](#)]
44. Huang, C.-N.; Chan, C.-T. A ZigBee-based location-aware fall detection system for improving elderly telecare. *Int. J. Environ. Res. Public Health* **2014**, *11*, 4233–4248. [[CrossRef](#)] [[PubMed](#)]
45. Rogers, N.C.; Seville, A.; Richter, J.; Ndzi, D.; Savage, N.; Caldeirinha, R.F.S.; Shukla, A.K.; Al-Nuaimi, M.O.; Craig, K.; Vilar, E.; et al. *A Generic Model of 1–60 GHz Radio Propagation through Vegetation—Final Report*; UK Radiocommunications Agency: Worcestershire, UK, 2002; p. 134.
46. Friis, H.T. A Note on a Simple Transmission Formula. *Proc. IRE* **1946**, *34*, 254–256. [[CrossRef](#)]
47. Afsharinejad, A.; Davy, A.; Jennings, B.; Rasmann, S.; Brennan, C. A path-loss model incorporating shadowing for THz band propagation in vegetation. In Proceedings of the IEEE Global Communications Conference (GLOBECOM), San Diego, CA, USA, 6–10 December 2015. [[CrossRef](#)]
48. Zhang, W.; He, Y.; Liu, F.; Miao, C.; Sun, S.; Liu, C.; Jin, J. Research on WSN channel fading model and experimental analysis in orchard environment. In *IFIP Advances in Information and Communication Technology*; 369 AICT (PART 2); Springer: Berlin/Heidelberg, Germany, 2012; pp. 326–333. [[CrossRef](#)]
49. Mahesh, G.; Balachander, D.; Rao, T.R. RF propagation measurements in agricultural fields for Wireless Sensor Communications. In Proceedings of the IEEE International Conference on Circuit, Power and Computing Technologies (ICCPCT), Nagercoil, India, 20–21 March 2013; pp. 808–812. [[CrossRef](#)]
50. Rama Rao, T.; Balachander, D.; Tiwari, N. UHF short-range pathloss measurements in forest & plantation environments for wireless sensor networks. In Proceedings of the IEEE International Conference on Communication Systems (ICCS), Singapore, 21–23 November 2012; pp. 194–198. [[CrossRef](#)]

51. Agrawal, S.K.; Garg, P. Calculation of channel capacity and rician factor in the presence of vegetation in higher altitude platforms communication systems. In Proceedings of the 15th International Conference on Advanced Computing and Communications (ADCOM), Guwahati, India, 18–21 December 2007; pp. 243–248.
52. Galvan-Tejada, G.M.; Duarte-Reynoso, E.Q. Some guidelines to simulate wireless sensor networks in a propagation environment with non-uniform vegetation. *Int. J. Sens. Netw.* **2015**, *17*, 40–51. [[CrossRef](#)]
53. Wong, T.W. Electrical, magnetic, photomechanical and cavitational waves to overcome skin barrier for transdermal drug delivery. *J. Control. Release* **2014**, *193*, 257–269. [[CrossRef](#)]
54. Gay-Fernandez, J.A.; Cuinas, I. Peer to peer propagation in vegetation media for wireless sensor networks. In Proceedings of the IEEE Antennas and Propagation Society, AP-S International Symposium (Digest), Chicago, IL, USA, 8–14 July 2012. [[CrossRef](#)]
55. Tewari, R.K.; Swarup, S.; Roy, M.N. Radio Wave Propagation Through Rain Forests of India. *IEEE Trans. Antennas Propag.* **1990**, *38*, 433–449. [[CrossRef](#)]
56. Savage, N.; Ndzi, D.; Seville, A.; Vilar, E.; Austin, J. Radio wave propagation through vegetation: Factors influencing signal attenuation. *Radio Sci.* **2003**, *38*. [[CrossRef](#)]
57. Mestre, P.; Ribeiro, J.; Serodio, C.; Monteiro, J. Propagation of IEEE802.15.4 in vegetation. In Proceedings of the World Congress on Engineering (WCE), London, UK, 6–8 July 2011; Volume 2, pp. 1786–1791.
58. Anderson, C.R.; Volos, H.I.; Buehrer, R.M. Characterization of low-antenna ultrawideband propagation in a forest environment. *IEEE Trans. Veh. Technol.* **2013**, *62*, 2878–2895. [[CrossRef](#)]
59. Shaik, M.; Kabanni, A.; Nazeema, N. Millimeter wave propagation measurements in forest for 5G Wireless sensor communications. In Proceedings of the Mediterranean Microwave Symposium, Abu Dhabi, UAE, 14–16 November 2017. [[CrossRef](#)]
60. Ndzi, D.L.; Harun, A.; Ramli, F.M.; Kamarudin, M.L.; Zakaria, A.; Shakaff, A.Y.M.; Jaafar, M.N.; Zhou, S.; Farook, R.S. Wireless sensor network coverage measurement and planning in mixed crop farming. *Comput. Electron. Agric.* **2014**, *105*, 83–94. [[CrossRef](#)]
61. Khairunniza-Bejo, S.; Ramli, N.; Muharam, F.M. Wireless sensor network (WSN) applications in plantation canopy areas: A review. *Asian J. Sci. Res.* **2018**, *11*, 151–161. [[CrossRef](#)]
62. Zakaria, Y.; Ivanek, L. Propagation measurements and estimation of channel propagation models in urban environment. *KSII Trans. Internet Inf. Syst.* **2017**, *11*, 2453–2467. [[CrossRef](#)]
63. Oroza, C.A.; Zhang, Z.; Watteyne, T.; Glaser, S.D. A machine-learning-based connectivity model for complex terrain large-scale low-power wireless deployments. *IEEE Trans. Cogn. Commun. Netw.* **2017**, *3*, 576–584. [[CrossRef](#)]
64. Rahim, H.M.; Leow, C.Y.; Rahman, T.A. Millimeter wave propagation through foliage: Comparison of models. In Proceedings of the IEEE 12th Malaysia International Conference on Communications (MICC), Kuching, Malaysia, 23–25 November 2015; pp. 236–240. [[CrossRef](#)]
65. Cuiñas, I.; Gay-Fernández, J.A. A proposal on spatial diversity in emergency communications within forest environments. In Proceedings of the 8th European Conference on Antennas and Propagation (EuCAP), The Hague, The Netherlands, 6–11 April 2014; pp. 1295–1298. [[CrossRef](#)]
66. Balachander, D.; Rao, T.R.; Mahesh, G. RF propagation investigations in agricultural fields and gardens for wireless sensor communications. In Proceedings of the IEEE Conference on Information and Communication Technologies (ICT), Thuckalay, India, 11–12 April 2013; pp. 755–759. [[CrossRef](#)]
67. Rahman, N.Z.A.; Tan, K.G.; Omer, A.; Rahman, T.A.; Reza, A.W. Radio propagation studies at 5.8 GHz for point-to-multipoint applications incorporating vegetation effect. *Wirel. Pers. Commun.* **2013**, *72*, 709–728. [[CrossRef](#)]
68. Mani, F.; Oestges, C. A ray based method to evaluate scattering by vegetation elements. *IEEE Trans. Antennas Propag.* **2012**, *60*, 4006–4009. [[CrossRef](#)]
69. Chee, K.L.; Torrico, S.A.; Kurner, T. Foliage attenuation over mixed terrains in rural areas for broadband wireless access at 3.5 GHz. *IEEE Trans. Antennas Propag.* **2011**, *59*, 2698–2706. [[CrossRef](#)]
70. Meng, Y.S.; Lee, Y.H. Investigations of foliage effect on modern wireless communication systems: A review. *Prog. Electromagn. Res.* **2010**, *105*, 313–332. [[CrossRef](#)]
71. Mestre, P.; Serôdio, C.; Morais, R.; Azevedo, J.; Melo-Pinto, P. Vegetation growth detection using wireless sensor networks. In Proceedings of the WCE 2010—World Congress on Engineering, London, UK, 30 June–2 July 2010; Volume 1, pp. 802–807.

72. Sabri, N.; Aljunid, S.A.; Ahmad, R.B.; Malek, M.F.A.; Kamaruddin, R.; Salim, M.S. Wireless sensor network wave propagation in vegetation: Review and simulation. In Proceedings of the LAPC—Loughborough Antennas and Propagation Conference, Loughborough, UK, 12–13 November 2012. [CrossRef]
73. Rahman, N.Z.A.; Tan, K.G.; Rahman, T.A.; Idris, I.F.M.; Hamzah, N.A.A. Modeling of Dynamic Effect of Vegetation for Fixed Wireless Access System. *Wirel. Pers. Commun.* **2017**, *96*, 1329–1354. [CrossRef]
74. Zolertia. Z1 Datasheet. 2017. Available online: <http://github.com/Zolertia/Resources/wiki/RE-Mote> (accessed on 21 March 2019).
75. Cama-Pinto, A.; Piñeres-Espitia, G.; Comas-González, Z.; Vélez-Zapata, J.; Gómez-Mula, F. Design of a monitoring network of meteorological variables related to tornadoes in Barranquilla-Colombia and its metropolitan area. *Ingeniare* **2017**, *25*, 585–598.
76. Cama-Pinto, A.; Piñeres-Espitia, G.; Zamora-Musa, R.; Acosta-Coll, M.; Caicedo-Ortiz, J.; Sepúlveda-Ojeda, J. Design of a wireless sensor network for monitoring of flash floods in the city of Barranquilla Colombia. *Ingeniare* **2016**, *24*, 581–599.
77. Zennaro, M.; Bagula, A.; Gascon, D.; Noveleta, A.B. Long distance wireless sensor networks: Simulation vs. reality. In Proceedings of the 4th ACM Workshop on Networked Systems for Developing Regions, NSDR '10, San Francisco, CA, USA, 15 June 2010. [CrossRef]
78. Montoya, F.G.; Gómez, J.; Cama, A.; Zapata-Sierra, A.; Martínez, F.; De La Cruz, J.L.; Manzano-Agugliaro, F.A. Monitoring system for intensive agriculture based on mesh networks and the android system. *Comput. Electron. Agric.* **2013**, *99*, 14–20. [CrossRef]
79. Cama-Pinto, A.; Gil-Montoya, F.; Gómez-López, J.; García-Cruz, A.; Manzano-Agugliaro, F. Wireless surveillance sytem for greenhouse crops. *DYNA* **2014**, *81*, 164–170. [CrossRef]



© 2019 by the authors. Licensee MDPI, Basel, Switzerland. This article is an open access article distributed under the terms and conditions of the Creative Commons Attribution (CC BY) license (<http://creativecommons.org/licenses/by/4.0/>).